Chemistry & Biology
Article

Discovery and Characterization of the Laulimalide-Microtubule Binding Mode by Mass Shift Perturbation Mapping

Melissa J. Bennett,[1] Khaled Barakat,[2] J. Torin Huzil,[3] Jack Tuszynski,[3] and David C. Schriemer[1,*]
[1]University of Calgary, Department of Biochemistry and Molecular Biology, 3330 Hospital Drive NW, Calgary, AB T2N 4N1, Canada
[2]University of Alberta, Department of Physics, 11322-89 Avenue, Edmonton, AB T6G 2G7, Canada
[3]Cross Cancer Institute, Division of Experimental Oncology, 11560 University Avenue, Edmonton, AB T6G 1Z2, Canada
*Correspondence: dschriem@ucalgary.ca
DOI 10.1016/j.chembiol.2010.05.019

SUMMARY

Conventional approaches to site mapping have so far failed to identify the laulimalide binding site on microtubules. Using mass shift perturbation analysis and data-directed docking, we demonstrate that laulimalide binds to the exterior of the microtubule on β-tubulin, in a region previously unknown to support ligand binding and well removed from the paclitaxel site. Shift maps for docetaxel and laulimalide are otherwise identical, indicating a common state of microtubule stability induced by occupancy of the distinct sites. The preferred binding mode highlights the penetration of the laulimalide side chain into a deep, narrow cavity through a unique conformation not strongly populated in solution, akin to a "striking cobra." This mode supports the development of a pharmacophore model and reveals the importance of the C1–C15 axis in the macrocycle.

INTRODUCTION

Paclitaxel and its mimetics represent a standard of care in the treatment of solid tumors of the breast, ovary, and lung (de Bree et al., 2006; Henderson et al., 2003; Paz-Ares et al., 2008). These drugs bind to microtubules in a manner that distorts the dynamic assembly properties of this protein polymer, leading to mitotic arrest and variable cell fates, including apoptosis. The pivotal role of microtubules in cell division has rendered the assembly unit, the α/β-tubulin dimer, an enduring target for the development of chemotherapeutic drugs. Clinical inadequacies of the taxoids, including severe and persistent peripheral neuropathies, drug resistance, and vehicle-related toxicities, continue to drive new ligand development (Argyriou et al., 2008; Hunt, 2009; Singer et al., 2005). Unfortunately the diffuse nature of the taxoid binding site has presented roadblocks to pharmacophore modeling and rational ligand design (Nettles et al., 2004), prompting a search for alternative therapeutic entry points.

Studies with a new class of polyketide macrolide isolated from deep-sea sponges have proposed the existence of a nontaxoid site that, when bound, induces microtubule stabilization in a fashion similar to the taxanes (Gaitanos et al., 2004; Hamel et al., 2006; Pryor et al., 2002). Laulimalide, also known as fijianolide B (Figure 1), is representative of this new class of agents. Laulimalide has demonstrated extremely high potency against solid tumor cancer cell lines (Mooberry et al., 1999). It increases the density of interphase microtubules and causes the formation of thick, short microtubule bundles in the cytoplasm of interphase cells and abnormal mitotic spindles (Mooberry et al., 2004). This leads to G2/M arrest and eventual cell death. While the promise of a more effective alternative to paclitaxel exists, the clinical future of laulimalide as a monotherapy is uncertain. One study has demonstrated efficacy in a human colon cancer model and limited general toxicity (Johnson et al., 2007), while another has demonstrated severe toxicity and minimal tumor inhibition (Liu et al., 2007). However, in combination with other tubulin-targeting antimitotic agents it shows significant synergy at the level of cytotoxicity and antiproliferative activity (Clark et al., 2006). Although the mechanism of this synergy has yet to be established, it may derive from the combined effects on tubulin dynamics (Gapud et al., 2004; Hamel et al., 2006; Jordan and Wilson, 2004). The ligand class in general also appears less susceptible to P-glycoprotein (Pgp)-mediated drug resistance than the taxanes (Clark et al., 2006; Mooberry et al., 1999).

Collectively, these findings argue for the continued exploration of laulimalide and the minimization of adverse toxicological properties through ligand design. A thorough exploration will require knowledge of the ligand binding site and a detailed understanding of structure-activity relationships, to permit the development of analogs with altered toxicity profiles and optimized synergistic effects. In addition, the discovery of a novel site for induction of microtubule stability will provide new opportunities to study molecular mechanisms relevant to cell division, by offering a new set of chemical probes.

The identification of the paclitaxel binding site was achieved by tubulin structural analysis using electron crystallography, but this has not been successful to date for the identification of the laulimalide site (Thepchatri et al., 2005). Using displacement studies, laulimalide was unable to inhibit Flutax-2 (a fluorescent paclitaxel) or [^{3}H] paclitaxel from binding, but this simply indicates that binding is distinct from the paclitaxel site (Pryor et al., 2002). Early efforts in site identification have involved peloruside A, a ligand of the same class that has been shown to compete with laulimalide for binding to microtubules (Gaitanos et al., 2004). A computational study has suggested that

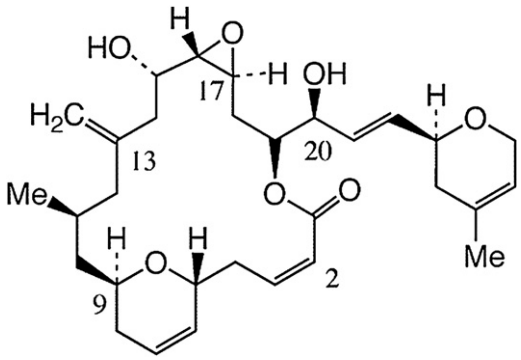

Figure 1. Chemical Structure of Laulimalide

peloruside A binds to the M-loop on α-tubulin in a region analogous to the paclitaxel site on β-tubulin (Jimenez-Barbero et al., 2006). However, a recent study in our lab proposed a site on β-tubulin on the exterior of the microtubule (Huzil et al., 2008). This was suggested upon an analysis of drug-induced microtubule stability using hydrogen/deuterium (H/D) exchange methods and mass spectrometry. An external site, if confirmed, would represent an obvious means by which endogenous protein regulators could affect microtubule stability in vivo.

The current study employs a refined mass spectrometry-based method to discover and characterize the laulimalide binding mode. The approach is inspired by chemical shift perturbation (CSP) methods in NMR, which are used extensively for protein interface mapping and more recently for protein-ligand interface mapping (Stark and Powers, 2008; Zuiderweg, 2002). In place of chemical shifts, ligand-induced perturbations of backbone amide H/D exchange rates are used as sensors for the formation of new interfaces and the allosteric effects of ligation. While H/D exchange mass spectrometry is used extensively in the study of protein folding (Engen, 2009; Maier and Deinzer, 2005), recent advancements promote the automated analysis of small molecule interactions with large molecular complexes, as well as extensive protein-protein interactions (Chalmers et al., 2006, 2007; Slysz et al., 2008, 2009). Here, we describe the application of this mass shift perturbation (MSP) method for laulimalide binding site determination, and, together with data-directed computational strategies, we present a high-resolution binding mode for the ligand on natural microtubule assemblies. Using MSP data, we also show that laulimalide induces a microtubule stability profile that is virtually indistinguishable from docetaxel and suggestive of a mechanism for synergy in tubulin assembly.

RESULTS

Mass Shift Perturbation Analysis of Ligated Microtubules

Replicate measurements of the ligand-induced perturbation of H/D exchange were conducted on assembled microtubules partially stabilized by a nonhydrolyzable analog of GTP (GMPCPP), to prevent depolymerization events during our analyses (Hyman et al., 1992). Ligand binding at the paclitaxel site induces further stabilization of microtubules, manifesting as reduced mass shifts in a large set of peptides monitored in the H/D exchange experiment (see Figures S1A and S1B available online), which is consistent with earlier findings (Huzil et al., 2008; Xiao et al., 2006). Experiments with laulimalide-stabilized microtubules revealed similarly extensive shift perturbations, rendering an objective localization of the binding site difficult (Figures S1C and S1D). We hypothesized that perturbations unique to the binding site could be detected more readily by suppressing common allosteric effects of ligand binding, using a stabilizer targeting the paclitaxel binding site. This was based on the observation that laulimalide binding is not competitive with fluorescent paclitaxel and does not appear to influence paclitaxel-tubulin stoichiometry (Pryor et al., 2002). To test this, microtubules were stabilized with a combination of laulimalide and docetaxel, the latter a hydroxylated paclitaxel binding to the taxoid site (Ringel and Horwitz, 1991). The resulting mass shift data were then compared with similar analyses of microtubules stabilized with each ligand separately and mapped to the regions in sequence space (Figure 2). We note that a direct comparison of shift data from laulimalide and docetaxel stabilized microtubules provides a similar opportunity, but referencing to a coligated, stabilized form provides reduced noise in the differential shift map and offers greater discrimination power (not shown).

The shift map arising from docetaxel applied to laulimalide-stabilized microtubules validates this strategy, as the taxoid binding site is clearly highlighted by large negative mass shifts (Figures 2A and 3B). This represents 7% of the peptides monitored, where docetaxel stabilization alone induced significant shifts in over 17% of peptides (Figure S1A). Two negative mass shifts arise from peptides defining a surface composed of the M-loop (β266–280) and the H6–H7 loop region (β213–230) (Figure 3A). The M-loop contains critical residues that are involved in the stabilization of the oxetane ring of the taxanes. In the H6-H7 loop region, Leu217 and Leu219 make hydrophobic contact with the 2-phenyl ring, assisting in stabilization (Lowe et al., 2001). As in an earlier study, the loop between βS9 and βS10 does not show significant labeling, even though this region appears in close contact with docetaxel based on established structures (Huzil et al., 2008).

Similarly, the shift perturbations arising from laulimalide applied to docetaxel-stabilized microtubules represent 5% of the peptides monitored (Figures 2C and 3B), where laulimalide stabilization alone caused shifts in at least 21% of the peptides (Figure S1C). Mapping this reduced set of perturbations to structure highlights a groove defined by the C-terminal ends of helices βH10 and βH9 on its sides and βH9' at its end (Figure 3B, boxed region). This region represents negative shifts for five overlapping peptides, defining a contiguous patch of solvent-accessible surface area that can be uniquely identified as the laulimalide binding site, as the allosteric effects of each ligand and their combination are identical under saturating conditions (see Supplemental Experimental Procedures). We note that the region encompasses the proposed site for peloruside A (Huzil et al., 2008).

Data-Directed Docking of Laulimalide

Computational routines for receptor-ligand modeling were then implemented to orient the ligand within the laulimalide binding site identified through the shift perturbation analysis. As the bound conformation of laulimalide is currently unknown, a large

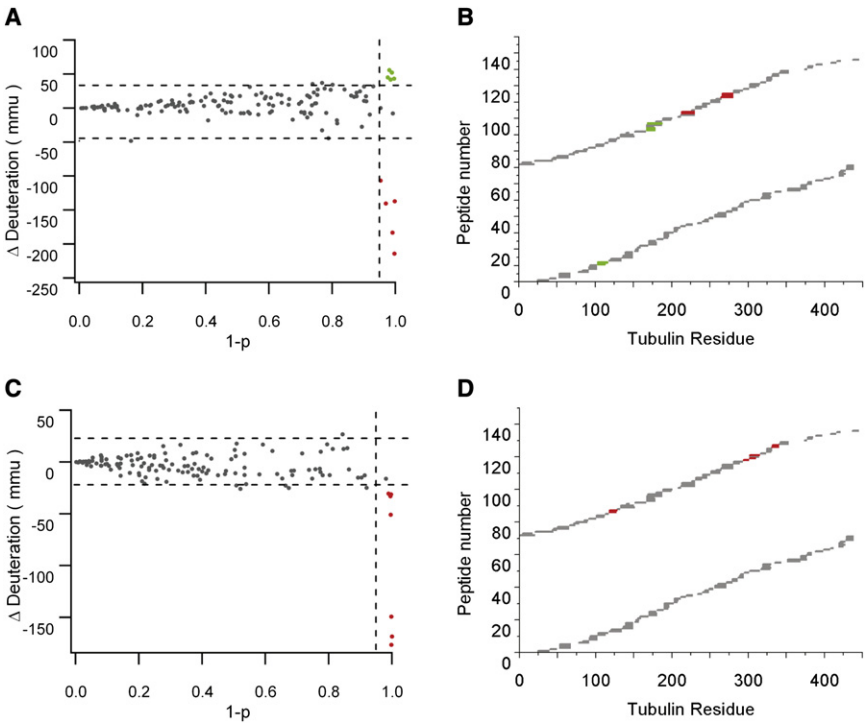

Figure 2. Mass Shift Perturbation Data between Singly and Doubly Ligated Microtubules

Mass shift perturbation data from analyses of doubly ligated microtubules relative to the singly ligated state.

(A) Scatterplot of replication MSP data for a comparison of doubly ligated microtubules with laulimalide-stabilized microtubules, highlighting the perturbations unique to docetaxel.

(B) Significant changes in (A) mapped to their locations in tubulin sequence.

(C) Scatterplot of replication MSP data for a comparison of doubly ligated microtubules with docetaxel-stabilized microtubules, highlighting the perturbations unique to laulimalide.

(D) Significant changes in (C) mapped to their locations in tubulin sequence. Each point in (A) and (C) represents the shift perturbation of a single peptide in millimass units (mmu). The horizontal dotted lines represent a ±2 SD cutoff based on noise in ΔD measurements and the vertical dotted line represents a 1-p cutoff value of 0.95. Green represents positive mass shifts resulting from single ligation and red represents negative mass shifts resulting from single ligation. The sequence maps (B and D) are arranged with α-tubulin on the bottom and β-tubulin on the top.

conformational library was generated that includes the 15 known solution conformers and an additional 1500 conformers generated from this starting set, to adequately sample the conformational space of the compound (see Experimental Procedures). These conformers were docked into an ensemble of tubulin structures to permit the sampling of a realistic degree of backbone diversity and principal side chain motions. As laulimalide binds to microtubules prestabilized with paclitaxel-site ligands, PDB entries 1JFF (Lowe et al., 2001), 1TUB (Nogales et al., 1998), and 1TVK (Nettles et al., 2004) were used for this purpose; these contain bound taxoid ligands. The set was supplemented with 1SA0 (Ravelli et al., 2004), which represents a colchicine and RB3/stathmin-stabilized tubulin structure.

The resulting poses for all conformers in the library were ranked by the lowest energy corresponding to the most populated cluster. That is, once all poses from each conformer entry were clustered, we filtered all of the clusters so that only those containing at least 25% of the total population are considered as top hits (Figure S2A), leading to the selection of two lowest energy binding modes, 1 and 2 (Figures S2B and S2C). The two modes have approximately inverted orientations within the groove, where mode 1 has a binding energy 2 kcal/mol lower than mode 2 based on AUTODOCK calculations. A blind docking exercise confirmed that these poses strongly favored the site identified by mass shift perturbation over any other region of the protein (e.g., Figure S3). There were no meaningful differences detected among the PDB entries with respect to the binding modes and binding energies.

MD Simulations and Refinement

MD simulations were then conducted from the lowest energy conformation for each mode. The trajectories of the simulations were used to perform an MM-PBSA analysis in order to calculate the relative binding energies and binding free energies (see Experimental Procedures). The two binding modes showed stability over the course of the simulation and neither deviated from the binding site or showed substantial fluctuations during the simulation. However, the MM-PBSA analysis (Table 1) highlights that mode 1 is strongly preferred over mode 2, returning binding free energies that correlate with solution data (Mooberry et al., 2004; Pryor et al., 2002). Consequently, mode 1 was used to determine the preferred conformation of the ligand within the binding site. We used clustering analysis to classify all possible binding poses into groups of similar conformations. To estimate the optimal number of clusters from the trajectory, this number was increased until sufficient convergence was achieved based on clustering metrics (see Experimental Procedures). Comparing the two metrics that were used in this study, a local minimum in DBI occurred at a cluster count of five. Although the SSR/SST ratio (where SSR is the sum-of-squares regression from each cluster summed over all clusters and SST is the total sum of squares ratio) did not saturate at this number of clusters, its value approached the convergence ratio. Thus, five clusters were taken to represent the laulimalide-tubulin simulation, where two of these clusters accounted for more than 75% of the whole trajectory. As the resulting poses from these two clusters are not significantly distinct from a structural perspective, the dominant one is shown in Figure 4. Finally, these simulations were also conducted in the presence of paclitaxel as stabilizer. Binding free energies were similar for the paclitaxel-free and paclitaxel-bound form although the enthalpy/entropy contributions were considerably different (Table 1). Upon coligation, laulimalide adopts a narrower profile within the binding site, although key receptor contacts are maintained (see below).

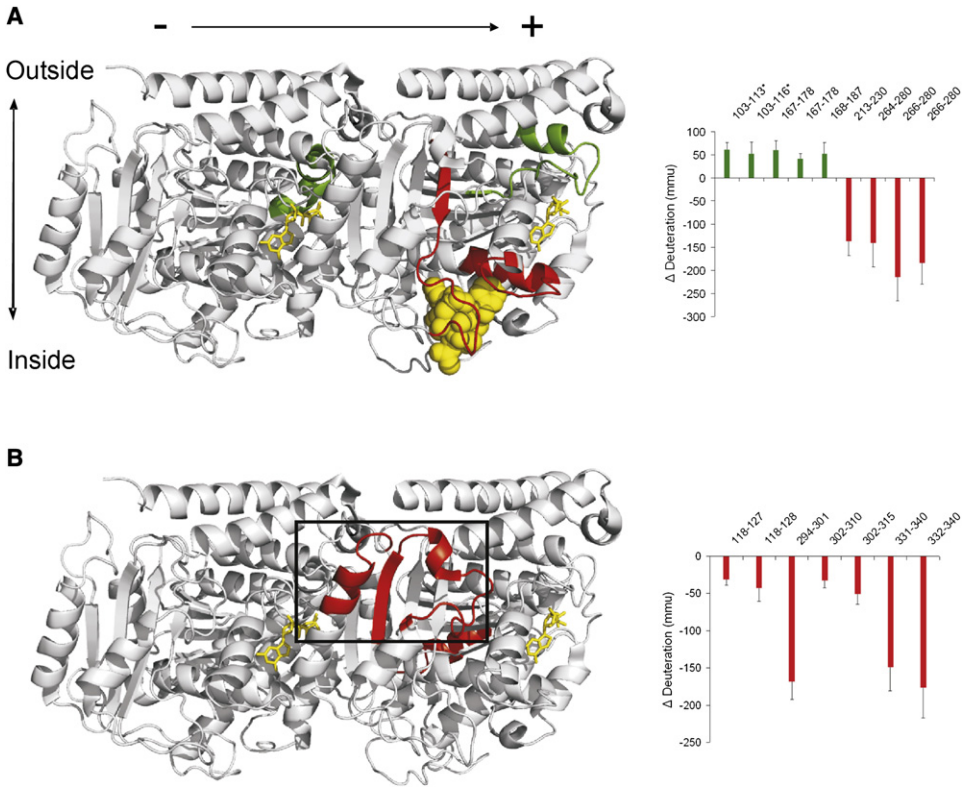

Figure 3. Differential MSP Data Mapped to α/β-Tubulin

Significantly perturbed mass shifts mapped to tubulin structure PDB 1JFF resulting from (A) docetaxel on a laulimalide-stabilized microtubule and (B) laulimalide on a docetaxel-stabilized microtubule. Corresponding histograms portray shift values per peptide (α-tubulin peptides shown with asterisk, ±1 SD). Red represents negative mass shifts and green positive mass shifts. Nucleotides are shown in yellow sticks, paclitaxel in yellow spheres, and the laulimalide site demarcated by the black square.

Coligation Shows Assembly Synergy and Does Not Affect Stoichiometry

A turbidometric assay confirmed that laulimalide and docetaxel act with positive overall synergy upon MT assembly under saturating conditions (Figure S4), as was noted in other combinations of laulimalide with taxoid site ligands (Hamel et al., 2006; Pryor et al., 2002). Additionally, coligation of laulimalide and docetaxel does not appear to influence the stoichiometry of binding. The mass shifts for peptides in both binding sites were compared relative to single ligand data and are equivalent, within the error of the measurements (Figure S5). As stoichiometry is 1:1 for each ligand separately, we conclude that under saturating conditions the interaction is 1:1:1 with respect to the ligands and assembled α/β-tubulin dimer. This is also consistent with earlier findings (Pryor et al., 2002). It remains possible that the dissociation constants are influenced upon coligation; however, this was not tested. A laulimalide titration experiment was conducted on free tubulin dimer, below the critical concentration for assembly. No measurable mass shifts were noted in the binding site up to 10 μM ligand (not shown), indicating that laulimalide binds preferentially to the assembled state, as with the taxoids (Diaz et al., 1993; Takoudju et al., 1988).

Table 1. Influence of Paclitaxel Binding on Possible Laulimalide Binding Modes

Mode[a]	A		B	
Paclitaxel[b] (with Zn^{2+})	Y	N	Y	N
Molecular mechanics energy	−37	−29	−21	−25
Entropy ($-TS_{Solute}$)	26	19	18	20
Binding free energy	−11	−10	−3	−5

[a] A-mode refers to "side chain in" orientation and B-mode to "side chain out" orientation. All energies in kcal/mol.

[b] Paclitaxel binding accompanied by Zn^{2+} to represent the PBD 1JFF tubulin structure (Lowe et al., 2001).

DISCUSSION

The potential of a new, nontaxoid entry point into mitotic regulation and cancer treatment has prompted vigorous activity to define a pharmacophore around laulimalide, in order to accelerate the development of clinically tractable analogs. To date, this has been ligand-based and indirect (Gollner et al., 2009), due to the lack of available structural information. There has been no report of a microtubule-laulimalide structure through crystallographic methods. While electron crystallography was used successfully for solving the paclitaxel-tubulin structure, there are challenges in the application of this technique to the solution of the laulimalide-tubulin structure, as it appears unable

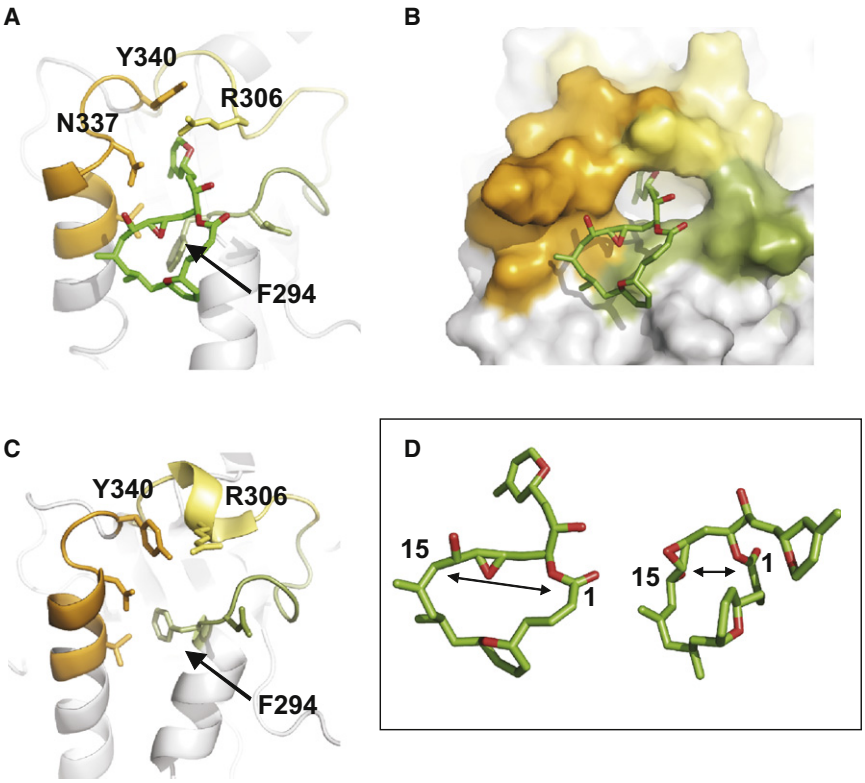

Figure 4. The Laulimalide-Tubulin Binding Mode Resulting from MSP-Guided Docking and Simulations

(A) The laulimalide pose resulting from MM-PBSA analysis, showing an intermolecular hydrogen bond to N337 and an intramolecular hydrogen bond between C20 OH and the carbonyl oxygen of the enoate.

(B) Surface representation of (A), highlighting the shallow groove under the macrocycle and the deep cavity surrounding the dihydropyran side chain. In both (A) and (B), three peptides representing MSP data are colored in orange, yellow, and green.

(C) The corresponding region from PBD entry 1JFF, highlighting the reorganization of F294, Y340, and R306 upon laulimalide binding in (A).

(D) Comparison of the bound conformer of this study (left) with the crystal structure for the free ligand (right) (Jefford et al., 1996). Oxygens are in red, and carbons are in green. The bound conformer is significantly elongated on the C1–C15 axis relative to the crystal structure, with the epoxide oriented into the macrocycle. The side chain orients into the page for the bound conformer, and out of the page for crystal structure. See also Figures S1 and S2.

to form the Zn^{2+}-stabilized sheets necessary for structure determination (Thepchatri et al., 2005).

To enable receptor-based pharmacophore modeling of complex protein systems, we have developed a mass spectrometric approach analogous to chemical shift perturbation (CSP) mapping by NMR, a method used extensively for interface mapping. Our method invokes limited deuterium uptake at amide bonds to facilitate rapid and accurate analysis of perturbed uptake (Slysz et al., 2008, 2009). We refer to this as "mass shift perturbation" (MSP) mapping. Data-directed docking strategies permit the orientation of the ligand within the region identified by the map. These maps are efficiently generated and mined from replicate data sets using ΔD – (1-p) plots (Figures 2A and 2C), to identify meaningful perturbations with accuracy.

This approach was used to identify the laulimalide binding site. As with NMR-based CSP data, ligand binding induces MSPs in the mass spectra through the creation of new interfaces as well as via allosteric effects (Englander et al., 2003; Mandell et al., 1998). It is not always clear, therefore, which region of the map represents the binding interface. This is the case for laulimalide-stabilized microtubules, where ligation led to a very large set of MSPs dispersed throughout the protein structure. The same is true of docetaxel, a hydroxylated analog of paclitaxel. A coligation strategy permitted a significant simplification of the MSP maps, enabling ready identification of the ligand binding sites for both ligands. This is possible as the endpoint of microtubule stabilization is obviously very similar between the two ligands, even though the binding sites are distinct. The localization of the laulimalide site to a groove defined by helices H9, H9', and H10 permitted a docking calculation into a much smaller volume, where the resulting gain in efficiency was distributed over a substantial sampling of laulimalide conformer space. This is a powerful means of implementing computational docking, leading to greater accuracy in interaction mapping as was recently demonstrated with NMR data (Stark and Powers, 2008).

A solution NMR study of laulimalide conformer space could not define a preferred orientation, as might be expected for a molecule with significant flexibility (Thepchatri et al., 2005). Upon docking and refinement by MD simulations, the binding mode described in the current study presents a conformer quite unique from the range presented in the study by Thepchatri et al. (2005). An RMSD (root mean square deviation) fitting of the bound form against all 15 conformers from Thepchatri et al. did not demonstrate a clear preference for any solution structure (not shown), although elements of a cobra motif are preserved for the macrocycle. The cobra has "struck" however, as the side-chain is deeply recessed within a long narrow cavity at the base of the groove defining the site, in an orientation preserving elements of the stretch motif (Figure 4A).

Although the binding groove exists within PDB 1JFF, which is a paclitaxel-stabilized tubulin structure, the site is reoriented upon binding of laulimalide and defines two notable regions (cf. Figures 4A and 4C). The macrolactone ring is positioned above a set of hydrophobic residues involving helices H9 and H10, which adopt a parallel, shifted orientation relative to the nonliganded form. This promotes improved packing of V333 and F294, where a 90° reorientation of the F294 phenyl group establishes the entrance to a deep cavity. The conformation of the macrolactone departs significantly from any of the solution conformers previously reported with the exception of the higher

energy cobra motif (Thepchatri et al., 2005). Examples of this motif exhibit an increased width of the macrolactone ring, as measured by the distance along the C1–C15 axis. The macrolactone ring of the bound conformer is similarly elongated along this axis, seemingly facilitated by the inward orientation of the epoxide (Figure 4D). This leads to a near-maximal separation between the C15 hydroxyl and the enoate. There are no obvious polar contacts involving the epoxide or the C5–C9 trans-dihydropyran of the macrolactone, suggesting that the binding energy contributed by this ring structure is primarily based on van der Waals contacts.

Ligand binding also promotes a reorganization of the side chains, providing a well-defined entrance to the narrow cavity. Both R306 and Y340 rearrange to establish a cation-pi interaction (Gallivan and Dougherty, 1999), promoting the stabilization of the loops in this region and presenting an orientation of R306 sufficient to generate polar contacts with the oxygen of the dihydropyran, in the laulimalide side chain. The hydroxyl group at C15 in laulimalide participates as a hydrogen bond acceptor with N337, a residue that also defines the entrance to the cavity. Interestingly, the C20 hydroxyl group of the side chain interacts with the C1 carbonyl oxygen of the enoate group via an internal hydrogen bond and does not appear to interact with D297. The internal hydrogen bond must be important in stabilizing the orientation of the side chain relative to the macrocycle, as a result. Validation of these findings through mutagenesis, though reasonable from a conceptual standpoint, is impractical for essential proteins such as α/β-tubulin. Previous attempts at generating recombinant α/β-tubulin has met with limited success (Katz et al., 1990; Sage et al., 1995; Shah et al., 2001). However, the binding site and the significance of the residues lining the cavity have been confirmed in a separate study of drug-selected mutants (D.L. Sackett, personal communication).

The MSP data set captures the critical contacts defined from the optimized docking model. Three nonoverlapping peptides define the site, as shown in Figure 4. The shifts cannot be associated with individual residues at this level of resolution, but the effect is unlikely to arise solely from altered solvent accessibility (Huyghues-Despointes et al., 1999). Stabilization of the underlying secondary structure upon binding would also perturb labeling, which is likely the case for R306 especially, where the host peptide does not experience any significant alteration in solvent accessibility at the backbone amides (not shown). It is interesting that the parallel site on α-tubulin does not appear to bind laulimalide, based on a blind docking experiment (Figure S3) and the absence of significant shift values in this region. A comparison of regions shows that, while secondary and tertiary structure are comparable, sequence similarity in the corresponding H10-loop region is poor and likely does not favor formation of an effective cleft for laulimalide side chain binding.

The laulimalide binding site is quite distinct from the paclitaxel binding site in its properties. While both share an underlying hydrophobic surface stabilizing a significant portion of the ligand, the paclitaxel site is considerably more diffuse, contributing to a overall ''promiscuity'' in binding modes and lack of a clearly defined pharmacophore (Nettles et al., 2004). Several ligands of remarkably varied structure bind with high affinity to the taxoid site. The laulimalide site appears to be well defined, smaller, and, as existing structure-activity data have shown, less tolerant of significant structural adaptations. While the shallow hydrophobic groove may be permissive of structural variation, the regions in and near the cavity clearly are not. This is affirmed by recent evidence highlighting the contribution of the side chain to activity (Gollner et al., 2009; Mooberry et al., 2008). The surprising role of the side chain can be understood based on dihydropyran interactions with R306 and the steric requirements of the cavity. For example, replacing the dihydropyran with a cyclohexane dramatically reduced activity in cytotoxicity assays (Wender et al., 2006). Nearly all modifications to the side chain have a similarly potent and negative effect on activity (Mooberry et al., 2008). The importance of the C20 hydroxyl group has been established by a number of labs. Modifications of this group have been explored in order to reduce its role in destabilizing the epoxide; however, a simple modification to a methoxy group reduces potency by two orders of magnitude (Gallagher et al., 2004). This highlights the importance of the internal hydrogen bond to the enoate, which we suggest confers conformational stability upon the ligand. Isolaulimalide, an analog with the C20 hydroxyl removed in order to promote the formation of a des-epoxy structure (Mooberry et al., 2004), is likely a poor ligand for a similar reason. An acetoxy modification reduces activity as well but not as strongly, perhaps due to compensating interactions with D297. The participation of the enoate in a stabilizing interaction with the C20 hydroxyl offers a reason why enoate modifications have a significant negative influence on activity (Gallagher et al., 2004).

Our structural model further points to the significance of the C15 hydroxyl group, which is also consistent with available structure-activity data. Replacing the hydroxyl with an acetoxy group has the mildest effect of all known modifications, as hydrogen bonding to N337 is likely preserved. As the C15 resides outside of the cavity, it is more tolerant of bulky substituents such as p-nitrobenzoate (Gallagher et al., 2004). Overall, a general pharmacophore model emerges where the side chain provides selectivity to the interaction and stabilizes a ring conformer through a critical internal hydrogen bond. This permits a positioning of the C15 hydroxyl group for favorable hydrogen bonding to N337, requiring a ''stretch'' along the C1–C15 axis of the macrolactone.

This study defines the first stabilizing binding site on microtubules that is fully removed from the taxoid site. All previously described small molecule stabilizers are in some way accommodated within the expansive taxoid binding site within the lumen of the microtubule, with the possible exception of cyclostreptin. This has been shown recently to transiently occupy a type I pore, but nevertheless still overlaps with the taxoid site on the lumenal side (Buey et al., 2007). The laulimalide site is located close to the intradimer interface and directly above the colchicine binding site (Figure 5). While it binds in the vicinity of a type II pore on the lattice, it would not require a fenestration event as is likely the case for taxoids (Diaz et al., 2003), and thus the site would be accessible to microtubule-associated proteins (MAPs). We note further that the laulimalide binding site is adjacent to the MAP-binding C-terminal E-hook on β-tubulin, and therefore this site may play a role in mediating MAP-tubulin interactions.

Although the laulimalide site is well removed from the taxoid site, occupancy at either site induces the same stabilization state, as reflected in the identical allosteric shift maps for both

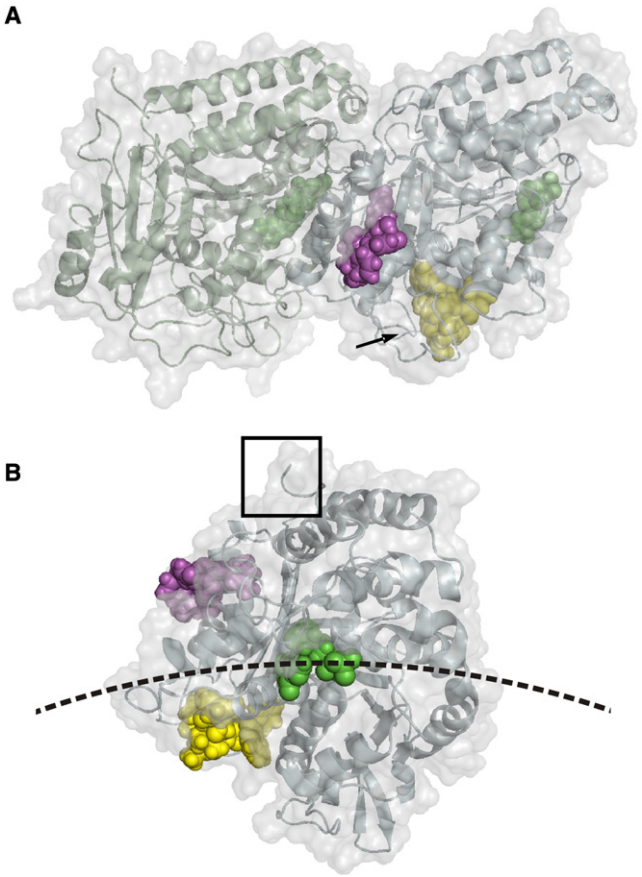

Figure 5. Orientation of Laulimalide Relative to Paclitaxel

(A) On the full-length α/β-tubulin dimer, plus end on the right, with the M-loop indicated with an arrow, and (B) on β-tubulin oriented with the plus-end out of the page, showing an approximate position of the protofilament contacts (dashed arc) and the base of the E-hook (box). Laulimalide is shown in magenta, paclitaxel in yellow and bound nucleotides in green, α-tubulin in pale green, and β-tubulin in pale cyan.

laulimalide and docetaxel (Figure S1). These identical maps should not be taken to indicate an identical mechanism of stabilization as they represent an "endpoint" view of stabilization. In other words, even though the ligand-stabilized MTs are indistinguishable from the perspective of conformational dynamics, the two ligands may yet induce stability in different ways. There are at least two possible mechanistic interpretations. Although remote in a structural sense, the laulimalide site and the taxoid site are relatively close in sequence space; H9 of the laulimalide binding site is C-terminal to the M-loop, a critical component of the taxoid binding site (Figure 5). Therefore, binding of laulimalide may stabilize this loop sufficiently to permit improved protofilament contact as has been proposed for paclitaxel. In other words, laulimalide may invoke a nearly identical mechanism of stabilization. Alternatively, laulimalide may directly stabilize the intradimer interface. In a previous study, the stability of the latent laulimalide binding site in the free tubulin dimer was shown to be sensitive to E-site nucleotide occupancy, where GDP-binding destabilizes this site relative to GTP (Bennett et al., 2009). Occupation of this site may therefore return a more GTP-like state and reduced tension in the microtubule lattice. Different mechanisms of stabilization may provide the basis for the assembly synergy that is observed between these ligands (Gapud et al., 2004).

SIGNIFICANCE

This work confirms the existence and location of a fourth distinct ligand binding site within α/β-tubulin. The laulimalide site joins the ranks of the colchicine, vinca, and taxol binding sites, with properties that directly couple into microtubule assembly and stability. In this regard, the laulimalide site is unique in its exposure to the outside surface of the microtubule. Colchicine is buried within the intradimer interface and the vincas are buried at the interdimer interface. The taxoids occupy a site that is either partially or fully exposed to the lumen of the microtubule. Many microtubule associated proteins and nonspecific basic molecules are thought to interact electrostatically via the tubulin E-hook; however, reports exist of interactions mediated through nonelectrostatic interactions, suggesting alternative sites of interaction (Chernov et al., 2008). The laulimalide binding site may represent a key domain for such interactions, although this will require further investigation. More specifically, the mapping of the laulimalide site will aid in further analog development as this site is mined for a novel class of chemical probes and, ultimately, antimitotic therapies.

Finally, the MSP approach as described extends the concept of interface mapping, as popularized by the NMR-based chemical shift perturbation method, into highly complex protein organizations. Both methods are very sensitive to additional effects such as conformational changes, and both bear a complicated relationship between the shift and its structural basis. However, mapping is still possible using either method provided there is a means to discriminate between interfaces and allosteric effects (Zuiderweg, 2002). The MSP method strongly relaxes both the sample amount and purity requirements relative to CSP methods and should be applicable protein mixtures of higher complexity. In this context, future work will describe the application of MSP techniques to the interplay of microtubule regulatory proteins.

EXPERIMENTAL PROCEDURES

Microtubule Preparation and Mass Shift Perturbation Measurements

Purified bovine brain tubulin (Cytoskeleton Inc., cat. no. TL238-A, lot no. 753) was reconstituted in 12.5 μl nucleotide free buffer (20 mM KCl, 10 mM K-Pipes [pH 6.9]) to 200 μM and incubated at 37°C for 30 min to initiate polymerization. Microtubules were then pelleted at 16,000 g for 5 min and briefly washed with assembly buffer (1 mM GMPCPP, 100 mM KCl, 10 mM K-PIPES, 1 mM $MgCl_2$ [pH 6.9]) containing either docetaxel (125 μM), laulimalide (125 μM), docetaxel and laulimalide together (125 μM each), or simply the assembly buffer. A volume of assembly buffer (with or without ligand at the above concentrations) was then added, and the samples were placed on ice for 30 min to induce depolymerization, yielding a protein concentration of 60 μM. The samples were separated into four 10 μl fractions and held on ice until analysis. Prior to mass shift perturbation measurements, an aliquot was incubated at 37°C for 30 min to induce (or complete) tubulin polymerization. Sample temperature was reduced to 20°C over 1 min, and the protein was labeled with the addition of D_2O (25% v/v labeling) at this temperature for 4 min. Previous studies confirmed that labeling was essentially complete by this

time (Huzil et al., 2008). Labeling was quenched by adding the sample to a chilled slurry of immobilized pepsin (Pierce) in 0.1M glycine-hydrochloride (pH 2.3), and labeled tubulin was digested for 2.5 min on ice. Digestion was terminated upon centrifugation of the slurry, and an aliquot of the supernatant was injected into the LC-MS system for analysis, as described elsewhere (Huzil et al., 2008). All deuteration measurements were performed in quadruplicate. Sequence coverages of 94% for α-tubulin and 94% for β-tubulin were achieved for this study through the detection of 136 peptides, as described previously in detail (Bennett et al., 2009; Huzil et al., 2008). Residue numbering is based upon bovine α-tubulin isoform I-C (UniProt P81948) and bovine β-tubulin isoform II-B (UniProt Q6B856).

Data Analysis

Average deuterium incorporation for all verified peptide sequences was determined using Hydra, a software package developed in-house for interrogating large sets of LC-MS and LC-MS/MS data (Slysz et al., 2009). Ligand-induced mass shift perturbations were quantitated for all combinations of the microtubule control, laulimalide-stabilized, docetaxel-stabilized, and doubly stabilized microtubules. Shift perturbations were considered significant provided the following criteria were met: passing a two-tailed *t* test ($p < 0.05$) using pooled standard deviations from quadruplicate analyses of each state; passing a distribution analysis to guard against spectral overlap (Chik et al., 2006); and exceeding a threshold shift value (±2 SD) based on a measurement of the shift noise and assuming its normal distribution. Selections were facilitated by the generation of two-dimensional ΔD versus 1-p plots. These plots aid in identifying peptides bearing significant shift data, avoiding determinations of significance on the basis of ΔD alone, and further serve to assess the overall quality of the MSP analysis.

The levels of altered deuteration were color coded per peptide on the linear sequence and the relevant tubulin structure (PDB 1JFF or resulting from MD simulations). Tubulin structures were rendered in all figures using Pymol (http://pymol.sourceforge.net). To determine the binding site for laulimalide, a comparison of the mass shift data arising from both the singly, and doubly ligated microtubules was formalized as described in the Supplemental Experimental Procedures.

Tubulin Assembly Assay

The assembly synergy of laulimalide and docetaxel on polymer assembly was investigated using 10 μM tubulin, the addition of laulimalide, and docetaxel individually (40 μM) and combined (20 μM each). Microtubule assembly was monitored turbidimetrically using a temperature controlled Varian Cary 50 UV-Vis spectrophotometer at 350 nm, following the method of Gapud et al., (2004). All assay components except ligand were added to a cuvette held at 10°C. Ligand was then added and assembly monitored for 1 hr at 10°C.

Laulimalide Conformer Library Generation and Conformer Docking

Absolute Cartesian coordinates for each of the fifteen solution conformers of laulimalide were obtained from supplementary information included in Thepchatri et al., (2005). These files were converted to xyz coordinates for subsequent import into JChem Standardizer (Chemaxon Inc.), where explicit hydrogen atoms and bond orders were set. These files were then exported into the mol2 format and imported into MarvinSketch (Chemaxon Inc.) using 3D transformation. The 15 seed conformers were subjected to conformer proliferation using the conformers tool in MarvinSketch. Default settings were chosen, the only exception being that the lowest energy conformer was not calculated, permitting instead the generation of 100 diverse conformers per starting conformer, producing a library of 1515 molecules for subsequent screening with AUTODOCK version 4.0. Details are provided in the Supplemental Experimental Procedures, including the procedure for blind docking of the top-ranked poses resulting from these activities.

Molecular Dynamics Simulations and Conformational Clustering

All Molecular Dynamics (MD) simulations were carried out using the NAMD program at a mean temperature of 310K and physiological pH (pH 7.0) using the all-hydrogen AMBER99SB force field. Details are provided in Supplemental Experimental Procedures. MD simulations on the laulimalide-tubulin complex produced numerous structures that explored its conformational space. A common approach to extract dominant conformations sampled during the MD simulation is to perform RMSD conformational clustering on the whole trajectory (Shao et al., 2007). To generate a reduced set of representative laulimalide-tubulin models, we performed RMSD conformational clustering with the average-linkage algorithm as implemented in the PTRAJ utility of AMBER10 using cluster counts ranging from 1 to 30 clusters. Structures were extracted at 2 ps intervals over the entire simulation. All C_α-atoms were RMSD fitted to the minimized initial structure in order to remove overall rotation and translation. RMSD-clustering was performed on laulimalide along with tubulin residues that are located within 10Å of the ligand. The selected system was clustered into groups of similar conformations using the atom-positional RMSD of all atoms, including side chains and hydrogen atoms, as the similarity criterion. The optimal number of clusters was chosen based on two clustering metrics, the Davies-Bouldin index (DBI) and the "elbow criterion" (Shao et al., 2007).

Binding Energy Analysis

Binding free energies were calculated using the molecular mechanics Poisson-Boltzmann surface area (MM-PBSA) method as implemented in AMBER10 and described in the Supplemental Experimental Procedures.

SUPPLEMENTAL INFORMATION

Supplemental Information includes Supplemental Experimental Procedures and five figures and can be found with this article online at doi:10.1016/j.chembiol.2010.05.019.

ACKNOWLEDGMENTS

We thank Dan L. Sackett for the provision of laulimalide and his helpful comments on the manuscript. This work was supported by the Canadian Institute for Health Research (D.C.S.), the Alberta Cancer Board (D.C.S., J.T.). D.C.S. gratefully acknowledges the additional support of the Canada Research Chair program and the Alberta Heritage Foundation for Medical Research (AHFMR). J.T. gratefully acknowledges the generous support of the Allard Foundation the Alberta Cancer Foundation, the National Sciences and Engineering Research Council (NSERC), and Alberta Advanced Education and Technology. All of the molecular dynamics simulations and virtual screening experiments were produced using the SHARCNET, AICT (University of Alberta cluster), and WESTGRID computational facilities. The authors declare no competing financial interests. M.J.B., J.T., and D.C.S. designed experiments; M.J.B., K.B., and J.T.H. conducted the research; M.J.B., K.B., and D.C.S. interpreted data; M.J.B. and D.C.S. wrote and edited the manuscript.

Received: February 9, 2010
Revised: May 6, 2010
Accepted: May 10, 2010
Published: July 29, 2010

REFERENCES

Argyriou, A.A., Koltzenburg, M., Polychronopoulos, P., Papapetropoulos, S., and Kalofonos, H.P. (2008). Peripheral nerve damage associated with administration of taxanes in patients with cancer. Crit. Rev. Oncol. Hematol. *66*, 218–228.

Bennett, M.J., Chik, J.K., Slysz, G.W., Luchko, T., Tuszynski, J., Sackett, D.L., and Schriemer, D.C. (2009). Structural mass spectrometry of the alpha beta-tubulin dimer supports a revised model of microtubule assembly. Biochemistry *48*, 4858–4870.

Buey, R.M., Calvo, E., Barasoain, I., Pineda, O., Edler, M.C., Matesanz, R., Cerezo, G., Vanderwal, C.D., Day, B.W., Sorensen, E.J., et al. (2007). Cyclostreptin binds covalently to microtubule pores and lumenal taxoid binding sites. Nat. Chem. Biol. *3*, 117–125.

Chalmers, M.J., Busby, S.A., Pascal, B.D., He, Y., Hendrickson, C.L., Marshall, A.G., and Griffin, P.R. (2006). Probing protein ligand interactions by automated hydrogen/deuterium exchange mass spectrometry. Anal. Chem. *78*, 1005–1014.

Chalmers, M.J., Busby, S.A., Pascal, B.D., Southern, M.R., and Griffin, P.R. (2007). A two-stage differential hydrogen deuterium exchange method for the rapid characterization of protein/ligand interactions. J. Biomol. Tech. *18*, 194–204.

Chernov, K.G., Mechulam, A., Popova, N.V., Pastre, D., Nadezhdina, E.S., Skabkina, O.V., Shanina, N.A., Vasiliev, V.D., Tarrade, A., Melki, J., et al. (2008). YB-1 promotes microtubule assembly in vitro through interaction with tubulin and microtubules. BMC Biochem. *9*, 23.

Chik, J.K., Vande Graaf, J.L., and Schriemer, D.C. (2006). Quantitating the statistical distribution of deuterium incorporation to extend the utility of H/D exchange MS data. Anal. Chem. *78*, 207–214.

Clark, E.A., Hills, P.M., Davidson, B.S., Wender, P.A., and Mooberry, S.L. (2006). Laulimalide and synthetic laulimalide analogues are synergistic with paclitaxel and 2-methoxyestradiol. Mol. Pharm. *3*, 457–467.

de Bree, E., Theodoropoulos, P.A., Rosing, H., Michalakis, J., Romanos, J., Beijnen, J.H., and Tsiftsis, D.D. (2006). Treatment of ovarian cancer using intraperitoneal chemotherapy with taxanes: from laboratory bench to bedside. Cancer Treat. Rev. *32*, 471–482.

Diaz, J.F., Menendez, M., and Andreu, J.M. (1993). Thermodynamics of ligand-induced assembly of tubulin. Biochemistry *32*, 10067–10077.

Diaz, J.F., Barasoain, I., and Andreu, J.M. (2003). Fast kinetics of Taxol binding to microtubules. Effects of solution variables and microtubule-associated proteins. J. Biol. Chem. *278*, 8407–8419.

Engen, J.R. (2009). Analysis of protein conformation and dynamics by hydrogen/deuterium exchange MS. Anal. Chem. *81*, 7870–7875.

Englander, J.J., Del Mar, C., Li, W., Englander, S.W., Kim, J.S., Stranz, D.D., Hamuro, Y., and Woods, V.L. (2003). Protein structure change studied by hydrogen-deuterium exchange, functional labeling, and mass spectrometry. Proc. Natl. Acad. Sci. USA *100*, 7057–7062.

Gaitanos, T.N., Buey, R.M., Diaz, J.F., Northcote, P.T., Teesdale-Spittle, P., Andreu, J.M., and Miller, J.H. (2004). Peloruside A does not bind to the taxoid site on beta-tubulin and retains its activity in multidrug-resistant cell lines. Cancer Res. *64*, 5063–5067.

Gallagher, B.M., Jr, Fang, F.G., Johannes, C.W., Pesant, M., Tremblay, M.R., Zhao, H., Akasaka, K., Li, X.Y., Liu, J., and Littlefield, B.A. (2004). Synthesis and biological evaluation of (-)-laulimalide analogues. Bioorg. Med. Chem. Lett. *14*, 575–579.

Gallivan, J.P., and Dougherty, D.A. (1999). Cation-pi interactions in structural biology. Proc. Natl. Acad. Sci. USA *96*, 9459–9464.

Gapud, E.J., Bai, R., Ghosh, A.K., and Hamel, E. (2004). Laulimalide and paclitaxel: a comparison of their effects on tubulin assembly and their synergistic action when present simultaneously. Mol. Pharmacol. *66*, 113–121.

Gollner, A., Altmann, K.-H., Gertsch, J., and Mulzer, J. (2009). Synthesis and biological evaluation of a *des*-dihydropyran laulimalide analog. Tetrahedron Lett. *50*, 5790–5792.

Hamel, E., Day, B.W., Miller, J.H., Jung, M.K., Northcote, P.T., Ghosh, A.K., Curran, D.P., Cushman, M., Nicolaou, K.C., Paterson, I., and Sorensen, E.J. (2006). Synergistic effects of peloruside A and laulimalide with taxoid site drugs, but not with each other, on tubulin assembly. Mol. Pharmacol. *70*, 1555–1564.

Henderson, I.C., Berry, D.A., Demetri, G.D., Cirrincione, C.T., Goldstein, L.J., Martino, S., Ingle, J.N., Cooper, M.R., Hayes, D.F., Tkaczuk, K.H., Fleming, G., et al. (2003). Improved outcomes from adding sequential Paclitaxel but not from escalating Doxorubicin dose in an adjuvant chemotherapy regimen for patients with node-positive primary breast cancer. J. Clin. Oncol. *21*, 976–983.

Hunt, J.T. (2009). Discovery of ixabepilone. Mol. Cancer Ther. *8*, 275–281.

Huyghues-Despointes, B.M., Scholtz, J.M., and Pace, C.N. (1999). Protein conformational stabilities can be determined from hydrogen exchange rates. Nat. Struct. Biol. *6*, 910–912.

Huzil, J.T., Chik, J.K., Slysz, G.W., Freedman, H., Tuszynski, J., Taylor, R.E., Sackett, D.L., and Schriemer, D.C. (2008). A unique mode of microtubule stabilization induced by peloruside A. J. Mol. Biol. *378*, 1016–1030.

Hyman, A.A., Salser, S., Drechsel, D.N., Unwin, N., and Mitchison, T.J. (1992). Role of GTP hydrolysis in microtubule dynamics: information from a slowly hydrolyzable analogue, GMPCPP. Mol. Biol. Cell *3*, 1155–1167.

Jefford, C.W., Bernardinelli, G., Tanaka, J., and Higa, T. (1996). Structures and absolute configurations of the marine toxins, latrunculin A and laulimalide. Tetrahedron Lett. *37*, 159–162.

Jimenez-Barbero, J., Canales, A., Northcote, P.T., Buey, R.M., Andreu, J.M., and Diaz, J.F. (2006). NMR determination of the bioactive conformation of peloruside A bound to microtubules. J. Am. Chem. Soc. *128*, 8757–8765.

Johnson, T.A., Tenney, K., Cichewicz, R.H., Morinaka, B.I., White, K.N., Amagata, T., Subramanian, B., Media, J., Mooberry, S.L., Valeriote, F.A., and Crews, P. (2007). Sponge-derived fijianolide polyketide class: further evaluation of their structural and cytotoxicity properties. J. Med. Chem. *50*, 3795–3803.

Jordan, M.A., and Wilson, L. (2004). Microtubules as a target for anticancer drugs. Nat. Rev. Cancer *4*, 253–265.

Katz, W., Weinstein, B., and Solomon, F. (1990). Regulation of tubulin levels and microtubule assembly in Saccharomyces cerevisiae: consequences of altered tubulin gene copy number. Mol. Cell. Biol. *10*, 5286–5294.

Liu, J.K., Towle, M.J., Cheng, H., Saxton, P., Reardon, C., Wu, J., Murphy, E.A., Kuznetsov, G., Johannes, C.W., Tremblay, M.R., et al. (2007). In vitro and in vivo anticancer activities of synthetic (-)-laulimalide, a marine natural product microtubule stabilizing agent. Anticancer Res. *27*, 1509–1518.

Lowe, J., Li, H., Downing, K.H., and Nogales, E. (2001). Refined structure of alpha beta-tubulin at 3.5 A resolution. J. Mol. Biol. *313*, 1045–1057.

Maier, C.S., and Deinzer, M.L. (2005). Protein conformations, interactions, and H/D exchange. Methods Enzymol. *402*, 312–360.

Mandell, J.G., Falick, A.M., and Komives, E.A. (1998). Identification of protein-protein interfaces by decreased amide proton solvent accessibility. Proc. Natl. Acad. Sci. USA *95*, 14705–14710.

Mooberry, S.L., Tien, G., Hernandez, A.H., Plubrukarn, A., and Davidson, B.S. (1999). Laulimalide and isolaulimalide, new paclitaxel-like microtubule-stabilizing agents. Cancer Res. *59*, 653–660.

Mooberry, S.L., Randall-Hlubek, D.A., Leal, R.M., Hegde, S.G., Hubbard, R.D., Zhang, L., and Wender, P.A. (2004). Microtubule-stabilizing agents based on designed laulimalide analogues. Proc. Natl. Acad. Sci. USA *101*, 8803–8808.

Mooberry, S.L., Hilinski, M.K., Clark, E.A., and Wender, P.A. (2008). Function-oriented synthesis: Biological evaluation of laulimalide analogues derived from a last step cross metathesis diversification strategy. Mol. Pharm. *5*, 829–838.

Nettles, J.H., Li, H.L., Cornett, B., Krahn, J.M., Snyder, J.P., and Downing, K.H. (2004). The binding mode of epothilone A on alpha,beta-tubulin by electron crystallography. Science *305*, 866–869.

Nogales, E., Wolf, S.G., and Downing, K.H. (1998). Structure of the alpha beta tubulin dimer by electron crystallography. Nature *391*, 199–203.

Paz-Ares, L., Ross, H., O'Brien, M., Riviere, A., Gatzemeier, U., Von Pawel, J., Kaukel, E., Freitag, L., Digel, W., Bischoff, H., García-Campelo, R., et al. (2008). Phase III trial comparing paclitaxel poliglumex vs docetaxel in the second-line treatment of non-small-cell lung cancer. Br. J. Cancer *98*, 1608–1613.

Pryor, D.E., O'Brate, A., Bilcer, G., Díaz, J.F., Wang, Y., Wang, Y., Kabaki, M., Jung, M.K., Andreu, J.M., Ghosh, A.K., Giannakakou, P., et al. (2002). The microtubule stabilizing agent laulimalide does not bind in the taxoid site, kills cells resistant to paclitaxel and epothilones, and may not require its epoxide moiety for activity. Biochemistry *41*, 9109–9115.

Ravelli, R.B., Gigant, B., Curmi, P.A., Jourdain, I., Lachkar, S., Sobel, A., and Knossow, M. (2004). Insight into tubulin regulation from a complex with colchicine and a stathmin-like domain. Nature *428*, 198–202.

Ringel, I., and Horwitz, S.B. (1991). Studies with RP 56976 (taxotere): a semisynthetic analogue of taxol. J. Natl. Cancer Inst. *83*, 288–291.

Sage, C.R., Davis, A.S., Dougherty, C.A., Sullivan, K., and Farrell, K.W. (1995). beta-Tubulin mutation suppresses microtubule dynamics in vitro and slows mitosis in vivo. Cell Motil. Cytoskeleton *30*, 285–300.

Shah, C., Xu, C.Z., Vickers, J., and Williams, R. (2001). Properties of microtubules assembled from mammalian tubulin synthesized in Escherichia coli. Biochemistry *40*, 4844–4852.

Shao, J., Tanner, S.W., Thompson, N., and Cheatham, T.E., III. (2007). Clustering molecular dynamics trajectories: 1. Characterizing the performance of different clustering algorithms. J. Chem. Theory Comput. *3*, 2312–2334.

Singer, J.W., Shaffer, S., Baker, B., Bernareggi, A., Stromatt, S., Nienstedt, D., and Besman, M. (2005). Paclitaxel poliglumex (XYOTAX; CT-2103): an intracellularly targeted taxane. Anticancer Drugs *16*, 243–254.

Slysz, G.W., Percy, A.J., and Schriemer, D.C. (2008). Restraining expansion of the peak envelope in H/D exchange-MS and its application in detecting perturbations of protein structure/dynamics. Anal. Chem. *80*, 7004–7011.

Slysz, G.W., Baker, C.A., Bozsa, B.M., Dang, A., Percy, A.J., Bennett, M., and Schriemer, D.C. (2009). Hydra: software for tailored processing of H/D exchange data from MS or tandem MS analyses. BMC Bioinformatics *10*, 162.

Stark, J., and Powers, R. (2008). Rapid protein-ligand costructures using chemical shift perturbations. J. Am. Chem. Soc. *130*, 535–545.

Takoudju, M., Wright, M., Chenu, J., Gueritte-Voegelein, F., and Guenard, D. (1988). Absence of 7-acetyl taxol binding to unassembled brain tubulin. FEBS Lett. *227*, 96–98.

Thepchatri, P., Cicero, D.O., Monteagudo, E., Ghosh, A.K., Cornett, B., Weeks, E.R., and Snyder, J.P. (2005). Conformations of laulimalide in DMSO-d(6). J. Am. Chem. Soc. *127*, 12838–12846.

Wender, P.A., Hilinski, M.K., Skaanderup, P.R., Soldermann, N.G., and Mooberry, S.L. (2006). Pharmacophore mapping in the laulimalide series: Total synthesis of a vinylogue for a late-stage metathesis diversification strategy. Org. Lett. *8*, 4105–4108.

Xiao, H., Verdier-Pinard, P., Fernandez-Fuentes, N., Burd, B., Angeletti, R., Fiser, A., Horwitz, S.B., and Orr, G.A. (2006). Insights into the mechanism of microtubule stabilization by Taxol. Proc. Natl. Acad. Sci. USA *103*, 10166–10173.

Zuiderweg, E.R. (2002). Mapping protein-protein interactions in solution by NMR spectroscopy. Biochemistry *41*, 1–7.

